

Modified Plastic-Damage Model for Fiber Reinforced Polymer-Confined Repaired Concrete Columns

I. A Tijani, Y. F Wu, C.W. Lim

Abstract—Concrete Damaged Plasticity Model (CDPM) is capable of modeling the stress-strain behavior of confined concrete. Nevertheless, the accuracy of the model largely depends on its parameters. To date, most research works mainly focus on the identification and modification of the parameters for fiber reinforced polymer (FRP) confined concrete prior to damage. And, it has been established that the FRP-strengthened concrete behaves differently to FRP-repaired concrete. This paper presents a modified plastic damage model within the context of the CDPM in ABAQUS for modelling of a uniformly FRP-confined repaired concrete under monotonic loading. The proposed model includes inflection damage, elastic stiffness, yield criterion and strain hardening rule. The distinct feature of damaged concrete is elastic stiffness reduction; this is included in the model. Meanwhile, the test results were obtained from a physical testing of repaired concrete. The dilation model is expressed as a function of the lateral stiffness of the FRP-jacket. The finite element predictions are shown to be in close agreement with the obtained test results of the repaired concrete. It was observed from the study that with necessary modifications, finite element method is capable of modeling FRP-repaired concrete structures.

Keywords—Concrete, FRP, damage, repairing, plasticity, and finite element method.

I. INTRODUCTION

DU E to a complex nature of concrete, a general and unified model has not been developed till date for the material. This is a major challenge in studying the behavior of concrete structures. Despite the complex nature of concrete, it is common belief that the primary behavior of concrete can be sufficiently captured by constitutive models based on the plasticity theory [1], [2].

Confining concrete structures with FRP is a suitable approach and recommended method for fast restoration of concrete ductility and strength [3]. However, Tsonos [4] divulged that FRP-strengthened concrete before damage behaves much differently from FRP-repaired concrete. Therefore, the parameters of FRP-retrofitted structures cannot be used in the calibration of the behavior of FRP-repaired structures [5], [6].

Plasticity-based models such as Drucker-Prager and CDPM are frequently adopted for the finite element analysis of FRP-conventional [7]. Extensive research has examined the plasticity behavior of FRP-retrofitted concrete [1], [8]-[13] to

I. A Tijani and C. W. Lim are with the Department of Architecture and Civil Engineering, City University of Hong Kong, Tat Chee Avenue, Kowloon, Hong Kong SAR and with the City University of Hong Kong Shenzhen Research Institute, Shenzhen 518057, P.R. China (e-mail: iatijani2-c@my.cityu.edu.hk, iatijani2-c@my.cityu.edu.hk).

Y. F Wu is with the School of Engineering, RMIT University, Melbourne, VIC 3000, Australia (e-mail: bccwlim@cityu.edu.hk).

mention a few. However, to best of the authors' knowledge, no study has examined the plasticity behavior of FRP-repaired concrete and identified the required modeling parameters.

For a plasticity model to satisfactorily capture and predict the behavior of confined concrete, the main features of plasticity model needs to be modified [9]. These features are (a) yield criterion; (b) a hardening/softening rule; and (c) a flow rule. The parameters of CDPM were extensively scrutinized by analyzing the obtained test results, and models for each parameter are developed, leading to a modified CDPM model for FEA of FRP-repaired concrete columns.

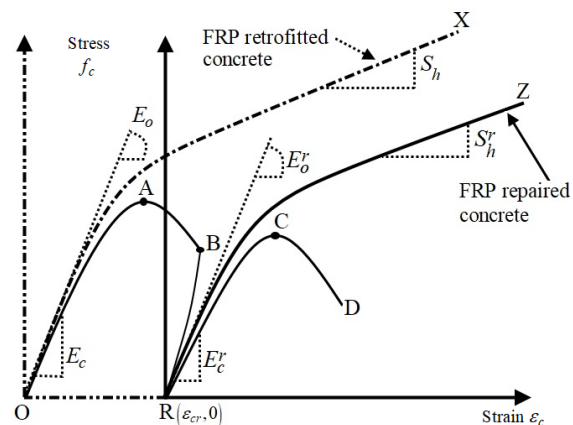


Fig. 1 Typical stress-strain curves for FRP-retrofitted and FRP-repaired concrete

II. TYPICAL STRESS-STRAIN RELATIONSHIP FOR PRE-LOADING, UNLOADING AND REPAIR PATH

Assume a plain concrete without pre-damage is monotonically loaded to point A following the path O-A-B, as in Fig. 1. Then, the loading is stopped, and the column is fully unloaded to point R and the repairing process was performed. Path R-C-D shows the stress-strain curve of unconfined repaired concrete, while the curve of FRP repaired concrete is depicted with path R-Z. Meanwhile, it is evident that a concrete column jacketed at point O is the conventional FRP confined concrete which the stress-strain curve follows the path O-X. The degree of the damage of the plain concrete increases as the load moves along the path O-A-B. The Young's modulus of plain and repaired concretes are indicated with E_c and E_c^{rd} , respectively, the initial modulus of FRP-retrofitted and FRP-repaired concretes are indicated with E_o and E_o^r , while the slope of the hardening part of FRP-

retrofitted and FRP-repaired concretes are indicated with S_h and S_h^r .

Damage degree of concrete δ is defined as the strength loss [5], [6]. Wu et al. [5] highlighted that the damage degree in (1a) is consistent with the damage variable adopted in continuum damage mechanics. The inflicted damage variable d^{id} is given in (1b).

$$\delta = 1 - f_{cd} / f_{co} \quad (1a)$$

$$d^{id} = 1 - \bar{A} / A \quad (1b)$$

where, f_{co} is the strength of undamaged concrete at point A in Fig. 1, f_{cd} is the peak remaining strength of unconfined repaired damage concrete at point C in Fig. 1, \bar{A} and A denote the total and effective cross-sectional areas of a member, respectively. FRP materials are brittle in nature and break immediately after reaching their strength [5]. Therefore, $f_{cd} / f_{co} = \bar{A} / A$. By substituting this expression in either (1a) or (1b), $d^{id} = \delta$. This parameter, d^{id} is later used for classical continuum damage mechanics.

II. EXPERIMENTAL PROGRAM

A short column cylinders of 150 mm in diameter and 300 mm in height were prepared and used in the current study. The experimental variables are concrete grade, damage degree, and FRP layers. The average undamaged and unconfined concrete strength was approximately 33.24 MPa and 51.79 MPa for C30 and C50 grades, respectively. On the other, the damage levels are 0%, 80%, 100%, -90%, -80%, -70%, -60% and -50% of the undamaged concrete strength. No visible crack was observed on the surface of the specimens with a positive damage degree for both concrete grades. Meanwhile, cracks are obvious on the specimens as the damage levels increasing down the descending part the stress-strain curve of plain concrete. The damage was inflicted using a compression machine of 1,600 kN capacity under a specified controlled displacement rate.

Sikadur-30, a solvent-free, thixotropic structural adhesive [5], was used to patched up the specimens with cracks, in order to have a smooth surface and friendly contact between the specimens and the FRP materials, the surface of the specimens with cracks was patched up with Sikadur-30. Subsequently, the specimens were wrapped with FRP materials. The confinement was performed 24 hours after the surface has been repaired. Although the internal cracks of the specimens with negative damage levels was not evident, thereby no injection of grout was attempted to seal the internal cracks; proper care was exercised not to disturb existing cracks of the specimen by keeping the specimen intact in its original vertical position during the wrapping process. Thereafter, the FRP-repaired concrete was subjected to

monotonic loading until failure using displacement control mode of approximately 15 kN/mm.

III. CDPM

Generally, the stress-strain response of the repaired concretes is bilinear with the second part of the curve as a linear revealing the ductile behavior of confined concrete. This response indicate that existing stress-strain relationship such as [3], [14]–[16] can captured the behavior of FRP confined repaired concrete. Therefore, it is deemed that the deformational behavior of FRP repaired concrete can be captured by a plasticity-based model on the condition that the material parameters are correctly identified and adjusted by experimental benchmarks.

A. Yield Criterion and Hardening Rule

When concrete is under a triaxial stress state a Drucker-Prager type of yield function [7], [9], [17] as given:

$$(1/3\gamma + 1)\bar{q} - (\gamma + 3\alpha)\bar{p} = (1 - \alpha)\bar{\sigma}_{cn}(\tilde{\varepsilon}_c^{rp}) \quad (2)$$

where \bar{p} and \bar{q} are the hydrostatic pressure and the Mises equivalent effective stress, defined in (3a) and (3b), respectively, $\bar{\sigma}_{cn}(\tilde{\varepsilon}_c^{rp})$ is the hardening parameter or effective cohesion stresses in compression, α , $\beta(\tilde{\varepsilon}^p)$, and γ are the dimensionless constants, which has been widely reported in existing studies [7], [9]. In the case of uniformly confined concrete, the hydrostatic pressure \bar{p} and the Mises equivalent effective stress \bar{q} are given as:

$$\bar{p} = \frac{\bar{\sigma}_c + 2\bar{\sigma}_l}{3} \quad (3a)$$

$$\bar{q} = \bar{\sigma}_c - \bar{\sigma}_l \quad (4b)$$

where $\bar{\sigma}_c$ and $\bar{\sigma}_l$ are the axial compressive stress and lateral confining pressure. Simplifying (2), we have:

$$\bar{\sigma}_{cn}(\tilde{\varepsilon}_c^{rp}) = \bar{\sigma}_c - \left(\frac{\gamma + 2\alpha + 1}{1 - \alpha} \right) \bar{\sigma}_l \quad (5)$$

The axial stress $\bar{\sigma}_c$ in (4) can be defined using Richart et al. [18], [19] empirical model.

$$\bar{\sigma}_c = f_{cd} + k_1 \bar{\sigma}_l \quad (6)$$

where, $\bar{\sigma}_{cn}(\tilde{\varepsilon}_c^{rp})$ is the hardening/cohesion parameter. Combining (4), and (5), we have:

$$\bar{\sigma}_{cn}(\tilde{\varepsilon}_c^{rp}) = f_{cd} + \left(k_1 - \frac{\gamma + 2\alpha + 1}{1 - \alpha} \right) \bar{\sigma}_l \quad (7)$$

The slope of hardening part is selected as critical parameter in identifying the hardening function of the repaired concrete. The slope of hardening S_h^r is obtained by:

$$S_h^r = \frac{\partial \bar{\sigma}_c(\tilde{\epsilon}_c^{rp})}{\partial \tilde{\epsilon}_c^{rp}} = \left(k_1 - \frac{\gamma + 2\alpha + 1}{1 - \alpha} \right) \frac{\partial \bar{\sigma}_i}{\partial \tilde{\epsilon}_c^{rp}} \quad (8)$$

B. Flow Rule

The flow rule is governed by the Drucker-Prager type plastic potential function G . The plastic strain increments can be obtained as:

$$d\epsilon_{ij}^{rp} = \lambda \frac{\partial G}{\partial \sigma_{ij}}$$

where

$$G = \sqrt{(\alpha \sigma_i \tan \psi)^2 + \bar{q}^2} - \bar{p} \tan \psi \quad (9)$$

where ϵ_{ij}^{rp} is plastic strain tensor, λ is the plastic multiplier coefficient, ψ is the plastic dilation angle, α is the eccentricity parameter equal to 0.1 [7], and σ_i is the failure uniaxial tensile stress. Two type of damage occurred in the present study. The first damage is inflicted damage d^{id} which occur prior to the repair at the point R in Fig. 1, while the second damage, compressive damage variable, d^{rd} occur after the repair process at point R. The initial stiffness of concrete E_c^{rd} at point R in Fig. 1 is given as:

$$E_c^{rd} = E_c \quad \text{when} \quad d^{id} = 0 \quad E_c^{rd} \neq E_c \quad \text{when} \quad d^{id} \neq 0 \quad (10)$$

where E_c is the undamaged modulus of concrete. The scalar damaged plastic strain is given as:

$$\tilde{\epsilon}_c^{rp} = \epsilon_c^r - \frac{1}{(1 - d^{id}) E_c^{rd}} (\sigma_c - 2\nu_c \sigma_l) \quad (11a)$$

$$\tilde{\epsilon}_l^{rp} = \epsilon_l^r - \frac{1}{(1 - d^{id}) E_c^{rd}} [(1 - \nu_c) \sigma_l - \nu_c \sigma_c] \quad (10b)$$

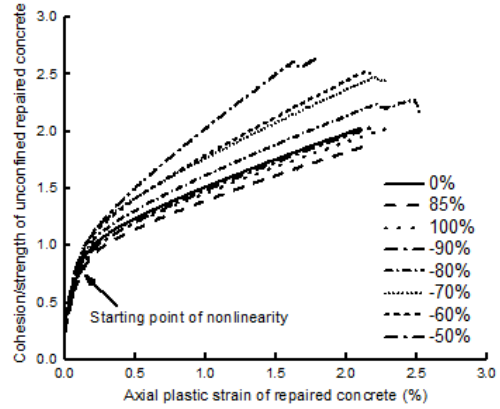
where ν_c is the Poisson's ratio of concrete, ϵ_c^r and ϵ_l^r are the axial and lateral strain of the repaired concrete, $\tilde{\epsilon}_c^{rp}$ and $\tilde{\epsilon}_l^{rp}$ are the axial and lateral plastic strain of repaired concrete.

IV. PARAMETER IDENTIFICATION

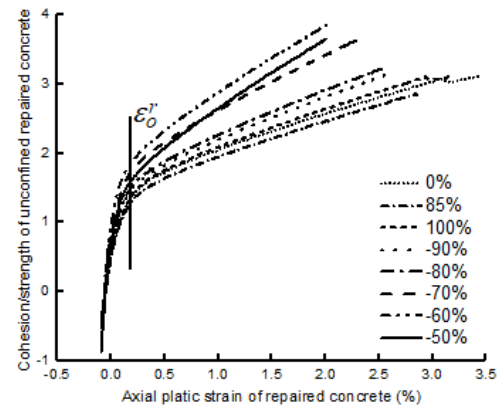
A. Hardening Parameter

A typical hardening curve of the repaired concrete is shown in Fig. 2. The hardening rate varies during the loading and it is

influenced by the lateral confinement stiffness ratio $\rho^r = 2E_f t_f / D f_{cd}$, where E_f , t_f denote the elastic stiffness and thickness of FRP materials, respectively, while D is the diameter of the specimen.



(a)



(b)

Fig. 2 Hardening curves as a function of f_{cd}

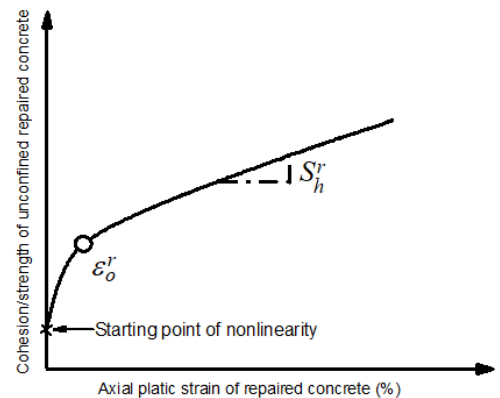


Fig. 3 General shape for hardening curve as a function of f_{cd}

Prior to the transition region ε_o^r , the repaired concrete dilation is insignificant. In this stage, the cohesion increase is mainly a function of f_{cd} as the confinement pressure is small. Meanwhile, after the point ε_o^r , the repaired concrete dilation and the resultant confinement pressure become significant. A typical hardening curve in Fig. 2 can be well illustrated by a general shape in Fig. 3.

The two parts hardening function depicted in Fig. 3 can be examined using (11) and the reported test results obtained from the confined repaired concrete. Therefore, the hardening function H^r is given as:

$$\begin{aligned} H^r &= \bar{\sigma}_{cn}(\tilde{\varepsilon}_c^{rp}) \quad \text{for } \tilde{\varepsilon}_c^{rp} < \varepsilon_o^r, \\ H^r &= \bar{\sigma}_{cn}(\tilde{\varepsilon}_c^{rp}) + S_h^r \quad \text{for } \tilde{\varepsilon}_c^{rp} \geq \varepsilon_o^r \end{aligned} \quad (12)$$

The region with $\tilde{\varepsilon}_c^{rp} < \varepsilon_o^r$ is slightly affected by the lateral stiffness ratio while the region $\tilde{\varepsilon}_c^{rp} \geq \varepsilon_o^r$ is significantly affected by lateral stiffness ratio. Therefore, $S_h^r = f(\rho^r)$. The curve part of the hardening prior to the region ε_o^r can be modeled using:

$$\bar{\sigma}_{cn}(\tilde{\varepsilon}_c^{rp}) = C_1 + C_2 \tilde{\varepsilon}_c^{rp} + C_3 (\tilde{\varepsilon}_c^{rp})^2 \quad (13)$$

By regressing the test data, the parameters C_1 , C_2 , and C_3 are determined and given as: $C_1 = 0.39$, $C_2 = 846.87$, and $C_3 = -358236.27$. Apparently, the value of ε_o^r does not affect the slope of the hardening part of the stress-strain curve. By regressing the slope S_h^r against ρ^r , a best fit line is determined, as shown in Fig. 4.

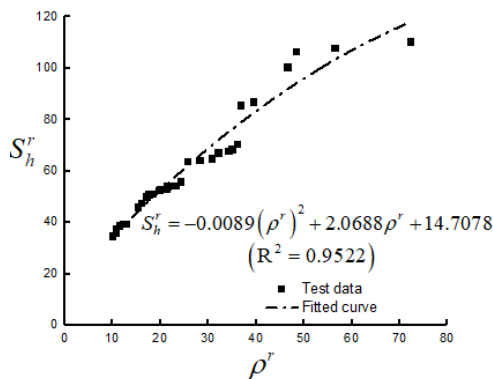


Fig. 4 Relationship between S_h^r and f_{cd}

The best fit equation is:

$$S_h^r = -0.0089(\rho^r)^2 + 2.0688\rho^r + 14.7078 \quad (14)$$

B. Dilation Parameter

The current study proposed a model for the plastic dilation angle ψ as a function of lateral stiffness ratio ρ^r , which is similar to the proposed model by other studies [7], [20]. By regressing the test data, the proposed model for ψ is given as:

$$\psi(\rho^r) = -1.32\rho^r + 53.05 \quad 0 \leq \rho^r \leq 40 \quad (15)$$

when $\rho^r = 0$, ψ is slightly less than 56.3, meanwhile, when $\rho^r = 40$, ψ is appropriately equals to 0.2. As shown in Fig. 5, the proposed model for ψ is compared to the function proposed by Mohammadi and Wu [7] and Hany et al. [20], as given in (15a) and (15b), respectively.

$$\psi(\rho) = -1.25\rho + 52.4 \quad (16a)$$

$$\psi(\rho) = -1.458\rho + 57.296 \quad (17b)$$

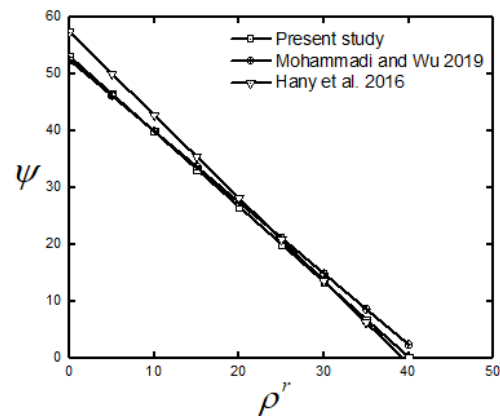


Fig. 5 Variation of plastic dilation angle ψ

V. PROPOSED MODEL VERSUS EXPERIMENTAL RESULTS

The proposed and modified plastic damage model for the FRP-confined repaired concrete is validated against experimental. Hany et al. [20] stated that compressive damage variable d^{rd} has a little effect on the stress-strain response of FRP confined concrete under monotonic loading, thereby the study neglected the effect of the variable. Therefore, the compressive damage variable d^{rd} is assumed to be zero. The specimens had a diameter of 150 mm, the unconfined repaired concrete strengths are 18.32 MPa and 40.21 MPa, with a corresponding strain of 2.23% and 2.04%, respectively. The FRP material had a tensile modulus of elasticity of 236 GPa and a thickness of 0.17 mm/ply. The finite element results are compared with the test results in Fig. 6. The predicted curves are terminated when the experimental ultimate hoop strain is reached.

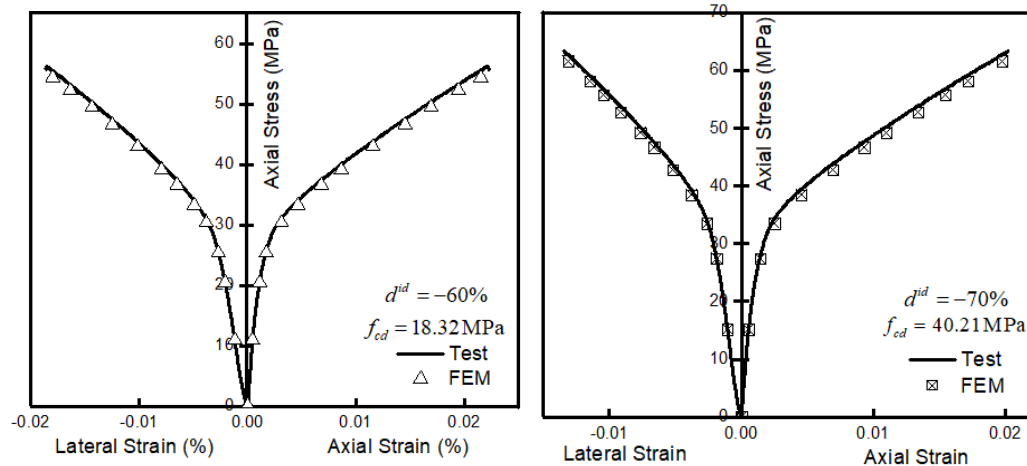


Fig. 6 Finite element results versus experimental results

VI. CONCLUSIONS

The hardening model is essential for finite element analyses of confined concrete using concrete damage plasticity model. An explicit model for the hardening and dilation parameters are developed in this work through analytical study of test results and finite element analysis by ABAQUS. The proposed model closely predicted the stress-strain response of the repaired concrete. This demonstrates the accuracy and effectiveness of the proposed modification.

ACKNOWLEDGMENTS

The work described in this paper was supported by Science Technology and Innovation Committee of Shenzhen Municipality (Project No. Basic 20170019) and City University of Hong Kong (Project No. 9680213).

REFERENCES

- Jiang, J. F. and Y. F. Wu, "Identification of material parameters for Drucker-Prager plasticity model for FRP confined circular concrete columns," *Int. J. Solids Struct.*, vol. 49, no. 3-4, pp. 445-456, Feb. 2012.
- Pekau, A. O., Z. X. Zhang, and G. T. Liu, "Constitutive model for concrete in strain space," *J. Eng. Mech.*, vol. 118, pp. 1907-1927, 1992.
- Tijani, I. A., Y. F. Wu, and C. W. Lim, "Aggregate size effects and general static loading response on mechanical behavior of passively confined concrete," *Constr. Build. Mater.*, vol. 205, pp. 61-72, 2019.
- Tsonos, A. G., "Effectiveness of CFRP-jackets and RC-jackets in post-earthquake and pre-earthquake retrofitting of beam-column subassemblages," *Eng. Struct.*, vol. 30, no. 3, pp. 777-793, Mar. 2008.
- Wu, Y.-F., Y. Yun, Y. Wei, and Y. Zhou, "Effect of predamage on the stress-strain relationship of confined concrete under monotonic loading," *J. Struct. Eng.*, vol. 140, no. 12, p. 04014093, Dec. 2014.
- Li, P., L. Sui, F. Xing, M. Li, Y. Zhou, and Y.-F. Wu, "Stress-strain relation of FRP-confined predamaged concrete prisms with square sections of different corner radii subjected to monotonic axial compression," *J. Compos. Constr.*, vol. 23, no. 2, p. 04019001, 2019.
- Mohammadi, M. and Y.-F. Wu, "Modified plastic-damage model for passively confined concrete based on triaxial tests," *Compos. Part B Eng.*, vol. 159, pp. 211-223, Feb. 2019.
- Yu, T., J. G. Teng, Y. L. Wong, and S. L. Dong, "Finite element modeling of confined concrete-I: Drucker-Prager type plasticity model," *Eng. Struct.*, vol. 32, no. 3, pp. 665-679, Mar. 2010.
- Yu, T., J. G. Teng, Y. L. Wong, and S. L. Dong, "Finite element modeling of confined concrete-II: Plastic-damage model," *Eng. Struct.*, vol. 32, no. 3, pp. 680-691, Mar. 2010.
- Kabir, M. Z. and E. Shafei, "Plasticity modeling of FRP-confined circular reinforced concrete columns subjected to eccentric axial loading," *Compos. Part B Eng.*, vol. 43, no. 8, pp. 3497-3506, 2012.
- Shahawy, M., A. Mirmiran, and T. Beitelman, "Tests and modeling of carbon-wrapped concrete columns," *Compos. Part B Eng.*, vol. 31, no. 6-7, pp. 471-480, Oct. 2000.
- Karabinis, A. I. and P. D. Kioussis, "Effects of confinement on concrete columns: Plasticity approach," *J. Struct. Eng.*, vol. 120, no. 9, pp. 2747-2767, Sep. 1994.
- Jiang, J., Y. Wu, and X. Zhao, "Application of Drucker-Prager plasticity model for stress-strain modeling of FRP confined concrete columns," *Procedia Eng.*, vol. 14, pp. 687-694, 2011.
- Youssef, M. N., M. Q. Feng, and A. S. Mosallam, "Stress-strain model for concrete confined by FRP composites," *Compos. Part B Eng.*, vol. 38, no. 5-6, pp. 614-628, 2007.
- Zhou, Y. W. and Y. F. Wu, "General model for constitutive relationships of concrete and its composite structures," *Compos. Struct.*, vol. 94, no. 2, pp. 580-592, 2012.
- Hoshikuma, J., K. Kawashima, K. Nagaya, and A. W. Taylor, "Stress-strain model for confined reinforced concrete in bridge piers," *J. Struct. Eng.*, vol. 123, no. 5, pp. 624-633, 1997.
- Ozbakkaloglu, T., A. Gholampour, and J. C. Lim, "Damage-plasticity model for FRP-confined normal-strength and high-strength concrete," *J. Compos. Constr.*, vol. 20, no. 6, p. 04016053, 2016.
- Richart, F. E., A. Brandtzaeg, and R. L. Brown, "The failure of plain and spirally reinforced concrete in compression," *Bull. 190, Univ. Illinois, Eng. Exp. Station. Champaign*, 1929.
- Richart, F. E., A. Brandtzaeg, and R. L. Brown, "A study of the failure of concrete under combined compressive stresses," *Bull. 185, Univ. Illinois, Eng. Exp. Station. Champaign, IL*, 1928.
- Hany, N. F., E. G. Hantouche, and M. H. Harajli, "Finite element modeling of FRP-confined concrete using modified concrete damaged plasticity," *Eng. Struct.*, vol. 125, pp. 1-14, Oct. 2016.